Type 2 Corticotropin-Releasing Factor Receptor in the Ventromedial Nucleus of Hypothalamus Is Critical in Regulating Feeding and Lipid Metabolism in White Adipose Tissue

Hongxia Chao, Michael Digruccio, Peilin Chen, and Chien Li

Department of Pharmacology, University of Virginia, Charlottesville, Virginia 22903

Ventromedial nucleus of hypothalamus (VMH) plays a critical role in regulating feeding and energy metabolism. The nucleus expresses high levels of the type 2 corticotropin-releasing factor receptor (CRFR2) and receives prominent innervation of nerve fibers containing Urocortin 3 (Ucn 3), an endogenous ligand of the receptor. In the present study, we showed that mice deficient in Ucn 3 had elevated basal feeding and increased nocturnal food intake after overnight fasting compared with the wild-type (WT) littermates. The Ucn 3 null mice also had lower circulating insulin levels compared with those of the WT mice. Interestingly, the mutant mice maintained a comparable body weight with the WT littermates. Mice with reduced CRFR2 expression in the VMH by small hairpin RNA knockdown (KD) recapitulated feeding phenotypes observed in the Ucn 3 null mice. However, VMH CRFR2 KD mice gained significantly more weight than control mice. The weight gain was due to an accumulation of white adipose tissue (WAT) accompanied by reduced plasma free fatty acids and glycerol levels, increased respiratory quotients, and improved glucose tolerance. On the other hand, plasma insulin levels were comparable with the receptor KD and control mice. Furthermore, the expression of several genes, including hormone-sensitive lipase, was significantly reduced in the WAT of VMH CRFR2 KD mice compared with controls. These results indicate that Ucn 3 signaling through CRFR2 is a critical molecular mediator in the VMH in regulating feeding and lipid metabolism in WAT. **(*Endocrinology* 153: 166–176, 2012)**

Urocortin 3 (Ucn 3) is a member of the corticotropin-releasing factor (CRF) peptide family identified in humans and rodents (1, 2). It displays high affinity for the type 2 CRF receptor (CRFR2) with minimal affinity for the type 1 CRFR (CRFR1) (1, 2). Thus, Ucn 3 is considered an endogenous ligand for CRFR2. In the brain, Ucn 3-expressing neurons are primarily located in the hypothalamus and the amygdala (1, 3). In the hypothalamus, the majority of Ucn 3 positive neurons are found in the rostral part of the perifornical area with moderate levels of Ucn 3 positive cells found in the median preoptic nucleus (3). Ucn 3-immunoreactive nerve fibers and terminals are distributed mostly in the forebrain areas, including the hypothalamus and limbic system, where prominent Ucn 3 fibers are found in the lateral septum, amygdala, and the bed nucleus of stria terminalis (3). In the hypothalamus, Ucn 3 fibers predominately innervate the ventromedial nucleus of hypothalamus (VMH) with moderate levels of innervation found in the medial preoptic area and the ventral premammillary nucleus (3). In addition to the central nervous system, Ucn 3 is also expressed in a number of peripheral tissues, including the digestive tract, kidney, heart, adrenal gland, and pancreatic β-cells (4–7).

ISSN Print 0013-7227 ISSN Online 1945-7170
Printed in U.S.A.

doi: 10.1210/en.2011-1312 Received May 30, 2011. Accepted October 14, 2011.
First Published Online November 8, 2011

Abbreviations: BAT, Brown adipose tissue; CRF, corticotropin-releasing factor; CRFR1, type 1 CRFR; CRFR2, type 2 CRF receptor; CRR, counterregulatory response; DEXA, dual energy x-ray absorptiometry; EE, energy expenditure; eWAT, epididymal WAT; FFA, free fatty acid; GFP, green fluorescent protein; GTT, glucose tolerance test; HFD, high-fat diet; HSL, hormone-sensitive lipase; ITT, insulin tolerance test; KD, knockdown; KO, knockout; PPAR, peroxisome proliferator-activated receptor; shRNA, small hairpin RNA; SNS, sympathetic nervous system; TG, triglyceride; Ucn 3, Urocortin 3; UCP1, uncoupling protein 1; VMH, ventromedial nucleus of hypothalamus; WT, wild type; WAT, white adipose tissue.

Functional studies have suggested that Ucn 3 in the brain is involved in the regulation of energy balance. Central administration of Ucn 3 suppresses food intake, stimulates sympathetic nervous system (SNS) activity and elevates blood glucose levels (8–11). Furthermore, overexpression of Ucn 3 in the hypothalamus in mice results in an increase in energy expenditure (EE) (12). Site-specific injection studies have been carried out to determine brain areas responsible for mediating the effects of Ucn 3. Injection of Ucn 3 into the VMH, but not the paraventricular nucleus of hypothalamus or amygdala, mimics the effects of central Ucn 3 in feeding, SNS activity, and blood glucose levels (9, 13). Importantly, CRFR2 is expressed abundantly in the VMH (14, 15). These results argue that VMH is an important site that mediates the effects of Ucn 3 in energy homeostasis.

The VMH plays a critical role in regulating energy balance. Extensive studies have shown the importance of this nucleus in regulating appetite (13, 16–18), body weight (19, 20), thermogenesis (21, 22), and glucose homeostasis (23–25). Earlier studies have suggested that VMH is also involved in regulating peripheral lipid metabolism. Electrical stimulation of the VMH produces significant elevation of plasma levels of free fatty acids (FFA) and glycerol (26, 27). Moreover, VMH stimulation also leads to a decrease in respiratory quotient (28), which indicates an increase in lipid utilization. On the other hand, VMH lesions block fasting-induced lipolysis in white fat (29). The effect of VMH in circulating FFA and glycerol is believed to be mediated by the SNS (27). The molecular mediators in the VMH underlying the effect in lipid metabolism remain to be identified.

Based on functional and anatomical studies, we hypothesized that endogenous Ucn 3 is involved in regulating feeding and peripheral energy metabolism and that CRFR2 in the VMH is critical in mediating these effects. To test this hypothesis, we first compared feeding and key metabolic parameters between Ucn 3 null mice and their wild-type (WT) littermates. We then investigated the functional role of Ucn 3 signaling in the VMH by using a lentiviral vector expressing small hairpin RNA (shRNA) approach to knock down CRFR2 expression in the VMH. Our study reveals that endogenous Ucn 3 is important in regulating food intake, especially nocturnal feeding, and that this effect is mediated by CRFR2 in the VMH. We also provide important evidence to suggest that VMH CRFR2 plays a critical role in body weight homeostasis and lipid metabolism in white adipose tissue (WAT).

Materials and Methods

Animals

Mice bearing a targeted deletion of the Ucn 3 gene have been described elsewhere (30). The mutant mice were originally generated on a mixed C57BL/6J and 129/SvJ genetic background. Mice used for this study were backcrossed to C57BL/6J mice for eight generations and were housed under a 12-h light, 12-h dark cycle. For basal food intake experiment, male Ucn 3 and WT littermates were housed individually and fed with regular rodent chow, with food being weighed daily. For the VMH CRFR2 knockdown (KD) study, 10- to 12-wk-old male C57BL/6J mice (The Jackson Laboratory, Bar Harbor, ME) were acclimated for 1 wk before surgery. For fasting-induced feeding study, individually housed mice were food deprived overnight before given preweighed food. Their food intake was monitored at various time points for 24 h. All studies were approved by the University of Virginia Animal Care and Use Committee.

Lentiviral vector production

Five different shRNA target sequences against various regions of the mouse CRFR2 open reading frame were selected (Supplemental Table 1, published on The Endocrine Society's Journals Online web site at http://endo.endojournals.org), and shRNA against CRFR2 expressing cassettes driven by a U6 promoter were constructed and cloned into a lentiviral packaging vector (p156RRLsinPPtCMV-GFP-PREU3Nhe, kindly provided by Inder Verma, The Salk Institute, La Jolla, CA). The viral vector also expresses green fluorescent protein (GFP) under the control of a cytomegalovirus promoter, thus allowing identification of brain areas and neurons infected by the viral vector (31). In addition, a control vector containing a nontarget scrambled sequence (Supplemental Table 1) was also generated. CRFR2 shRNA vector or control vector and lentiviral packaging plasmids were cotransfected into HEK239FT cells (31). After transfection, the supernatant containing the viral particles was harvested, clarified, and concentrated by centrifugation. The ability of the shRNA viral vectors to knock down CRFR2 expression was first tested *in vitro* in A7r5 cells, an aortic smooth muscle cell line expressing endogenous CRFR2 (1, 32). Cells were infected with either CRFR2 shRNA or control viral vector, and CRFR2 mRNA levels in the cells were determined by real-time PCR. We found that shRNA-4 and shRNA-5 showed greatest reduction in CRFR2 mRNA compared with control vector-infected cells (Supplemental Fig. 1). shRNA-4 and shRNA-5 viral vector were further tested *in vivo* by injecting the viral vector or control vector unilaterally into the lateral septal nucleus, where abundant CRFR2 mRNA is expressed (14, 15). We found shRNA-5 greatly suppressed CRFR2 mRNA levels compared with the contralateral site, whereas shRNA-4 only showed modest reduction (data not shown). Thus, shRNA-5 was used for subsequent experiments to knock down CRFR2 in the VMH.

Stereotaxic injection

Mice anesthetized with a mixture of ketamine (80 mg/kg) and xylazine (8 mg/kg) were placed in a stereotaxic apparatus (David Kopf Instruments, Tujunga, CA), and CRFR2 shRNA or control lentiviral vector (0.1 μl/side) was delivered via a Hamilton syringe into the VMH [coordinates: from bregma (in millimeters) 1.42 caudal, 0.23 lateral, and 5.8 from the skull]. After surgery, animals were returned to the home cage and allowed to recover for 7–10 d before experiment. For chronic body weight and food intake measurements, a cohort of 24 mice was randomly divided into two groups with one receiving CRFR2 shRNA viral vector (CRFR2 KD) and the other group receiving control vector (con-

trol) injection into the VMH. Indirect calorimetry and dual energy x-ray absorptiometry (DEXA) scan were performed at the end of the monitoring period. Blood and tissue were collected from these mice at the end of the experiment for further analysis, and brains were processed for visualizing GFP and for *in situ* hybridization to measure CRFR2 mRNA. Six mice injected with CRFR2 shRNA viral vector and five injected with control vector were found to have misplaced injection sites (as determined by GFP expression and CRFR2 mRNA levels in the VMH) and were excluded from final analysis. A separate cohort of mice received CRFR2 shRNA or control vector (n = 10/group) injection and were used to monitor food intake, fasting-induced refeeding study, and glucose tolerance test (GTT) and insulin tolerance test (ITT). Four mice from each group were excluded from data analysis due to misplaced injection sites.

Indirect calorimetry and body composition

Food intake, ambulatory activity, oxygen consumption (VO_2), and CO_2 production were determined in an Oxymax metabolic chamber system (Columbus Instruments, Columbus, OH). Mice were placed in a chamber, and every 15 min, one reading per mouse was taken over 72 h. Mice were allowed to adjust to the cages during the first 24 h and thus only the last 48 h of each experimental run was used for data analysis. Resting metabolic rate was determined by measuring VO_2 for each animal during a 150-min period of inactivity. For body composition, DEXA measurement was performed after the EE assessment. Mice were anesthetized, introduced into the DEXA machine (Lunar Piximus II; GE Healthcare, Princeton, NJ), and subjected to total body imaging. Lean body mass and fat mass were determined using Lunar Piximus II software.

GTT and ITT

A GTT was performed in overnight-fasted mice after ip injection of 2 g/kg of body weight glucose. An ITT was conducted after 2 h of fasting with ip injection of insulin (0.75 IU/kg of body weight). Blood glucose levels were determined by a glucometer at various time points after glucose or insulin injection.

Plasma chemistry measurement

Blood glucose levels were measured from tail vein bleedings using a Nova Max blood glucose meter and test strips (Sanvita, Bedford, MA). Blood was collected from mice at the end of the experiments and quickly centrifuged at 4 C for 10 min. The plasma was collected and stored at −80 C for later analysis. Reagents used included: mouse endocrine panel for insulin, leptin, and glucagon (Millipore, Billerica, MA); Costicosterone RIA kit (MP Biomedicals, Solon, OH); Ultra sensitive 2-CAT ELISA kit (Rocky Mountain Diagnostics, Colorado Springs, CO); Free Glycerol Reagent (Sigma, St. Louis, MO); and nonesterified fatty acid kit (Wako Diagnostics, Richmond, VA). All assays were performed in duplicate with manufacturers' suggested protocols.

Real-time PCR analysis

Total RNA was extracted from epididymal WAT (eWAT), interscapular brown adipose tissue (BAT), liver, and muscle with Tri Reagent (Molecular Research Center, Cincinnati, OH). The quality of RNA was confirmed by ethidium bromide staining in 2% agarose gel. Gene sequences were obtained from the GenBank database. Primers were designed using IDT PrimerQuest or Primer 3 (Supplemental Table 2). Single-strand cDNA was synthesized using iScript cDNA Synthesis kits (Bio-Rad, Hercules, CA). PCR was performed using a MyIQ Single Color Real-Time PCR Detection System (Bio-Rad). Amplification products were verified by melting curves and agarose gel electrophoresis. All reactions were performed in duplicate. Values were normalized against 18S RNA or β-actin (33).

Histological analysis

Mouse eWAT samples were fixed in formalin, embedded in paraffin, and sectioned at 10-μm intervals. The sections were then stained with hematoxylin and eosin and coverslipped with permount. To examine the sizes of the white adipocytes, the adipocyte number was counted in five random areas (0.258 mm^2) of each stained specimen, and three sections per animal were counted.

In situ hybridization

Mouse brains were sectioned into one-in-four, 20-μm coronal sections, and the sections were then processed for *in situ* hybridization to detect CRFR2 mRNA as previously described (3). Briefly, a cRNA probe for mouse CRFR2 was transcribed from a linearized vector containing 460 bp of mouse CRFR2 cDNA in the presence of the ^{33}P-labeled uridine-5′-triphosphate (PerkinElmer, Waltham, MA). Brain sections were washed and then exposed to the cRNA probe overnight at 55 C. After incubation, brain sections were washed in saline-sodium citrate buffer, which increased in stringency, in ribonuclease, and in 0.1× saline-sodium citrate buffer at 60 C. Slides were then exposed to autoradiographic films (Bio-Max; Kodak, New York, NY) before being dipped in emulsion (Kodak) and incubated at 4 C for 14 d. They were then developed, stained with cresyl violet, and coverslipped with DPX mountant (Sigma).

Results from the *in situ* hybridization study were examined and captured by a Nikon 80i microscope coupled with a QImaging CCD camera (BioVision Technologies, Exton, PA) controlled by iVision software (BioVision). For data analysis, the coronal brain sections processed for the experiments were first anatomically matched across animals. Identification of the VMH area was aided by cresyl violet counterstain. CRFR2 mRNA-positive signals in the VMH were identified and counted in evenly spaced brain sections (~150- to 200-μm intervals). A neuron was considered to be positive if the number of silver grains on top of the cell body was three times greater than the background levels. On average, three to four sections that were evenly distributed across the rostrocaudal levels of the VMH were used for cell count. Results for each brain area are presented as mean ± SEM.

Statistical analysis

Data are expressed as mean ± SEM. The data normality of each outcome variable was first determined, and most variables satisfied the normality assumption. Data from accumulated food intake and refeeding studies required Box-Cox transformation for data normality. Statistical significance of each variable was evaluated using a Student's *t* test to compare the means of the two groups. The combined effects of genotypes (or treatment) and time on body weight changes, fasting-induced feeding, GTT, ITT, and accumulated food intake [Ucn 3 knockout (KO) *vs.* WT] were analyzed using a two-way ANOVA with repeated measurements over time.

Results

Ucn 3 mutant mice displayed elevated basal food intake compared with the WT littermates while maintaining comparable body weight as WT mice

To evaluate the physiological significance of endogenous Ucn 3 in regulating energy balance, the body weight of male Ucn 3 null mice and WT littermates was followed for 14 wk (wk 6–20). As shown in Fig. 1A, the Ucn 3 mutant and the WT mice exhibited similar body weight throughout the experimental period. Postmortem analysis found similar weight in major organs between the two genotypes (data not shown). Basal food intake was measured daily from wk 12 to 18. Ucn 3 mutant mice consistently showed a significant increase in food intake than the WT littermates (Fig. 1B). In addition, accumulated food intake of the Ucn 3 mutants during this period was significantly higher than that of the WT mice (Fig. 1C). Two-way ANOVA with repeated measurement showed significant effects of genotype [$F_{(1,18)} = 6.4$, $P = 0.02$] and interaction between genotype and time [$F_{(5,90)} = 49.6$, $P < 0.001$] on accumulated food intake.

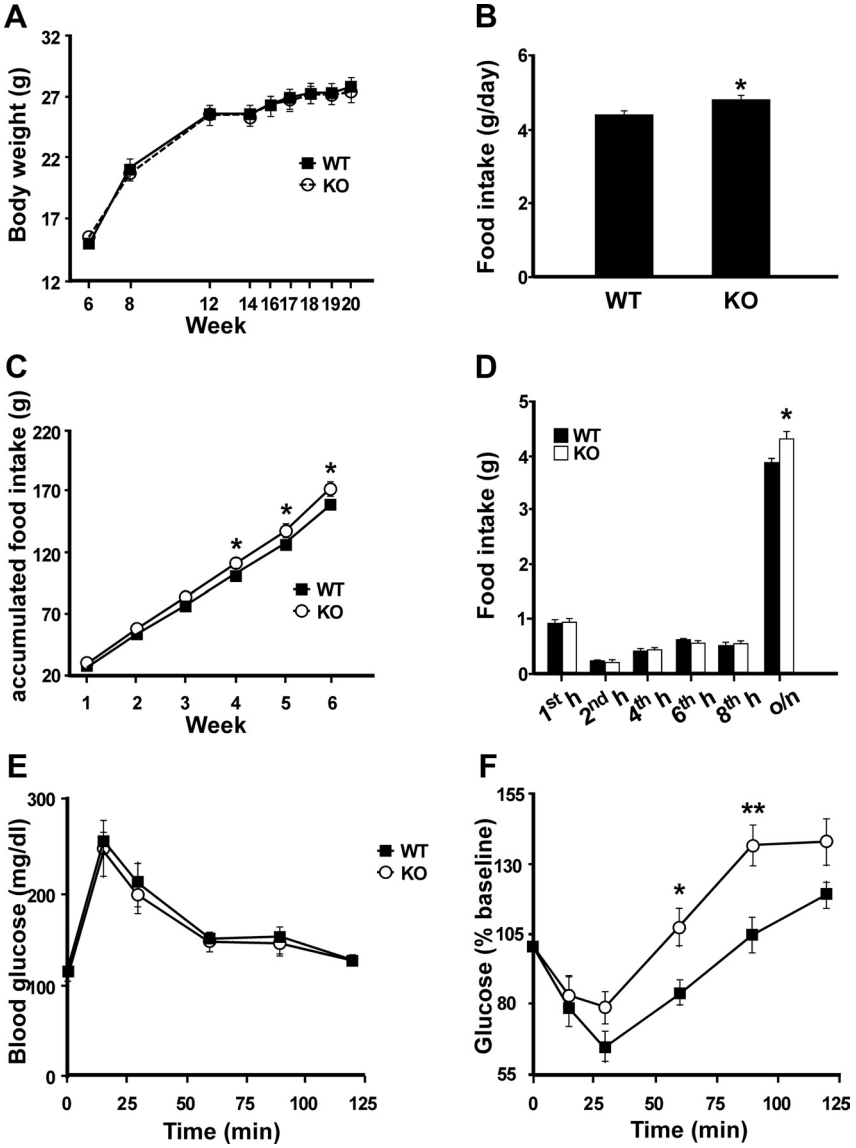

FIG. 1. Characterization of Ucn 3 null mice. A, Body weight of male Ucn 3 KO (n = 10) and WT (n = 10) mice from wk 6 to 20. B, Average daily food intake of male Ucn 3 KO and WT littermates between wk 12 and 18. C, Accumulated food intake of Ucn 3 null mice and WT mice between wk 12 (first week) and 18 (sixth week). D, Overnight fasting-induced feeding in Ucn 3 null (KO) and WT littermates. Male Ucn 3 KO mice (n = 10) and WT mice (n = 10) were food deprived overnight and then food intake was measured 1, 2, 4, 6, 8, and 24 h after food was returned to the animals. E and F, GTT (E) and ITT (F) in Ucn 3 null (n = 7) and WT mice (n = 9). Glucose (2 g/kg body weight) or insulin (0.75 IU/kg body weight) was injected ip, and blood glucose was measured at various time points. Note the Ucn 3 null mice had an exaggerated hyperglycemic rebound compared with the WT mice. **, $P < 0.01$; *, $P < 0.05$ *vs.* WT littermates. o/n, Overnight.

Fasting-induced feeding in Ucn 3 mutant mice and WT littermates

The importance of endogenous Ucn 3 in regulating feeding was also assessed in an overnight fasting-induced feeding paradigm. Two-way ANOVA analysis with repeated measurement found that food intake was independent of genotype [$F_{(1,18)} = 4.17$, $P = 0.06$]. However, a significant genotype by time interaction was found on refeeding response [$F_{(5,90)} = 2.64$, $P = 0.028$]. Both the mutant and WT mice ate a similar amount of food at 1, 2, 4, 6, and 8 h after onset of feeding, but the Ucn 3 null mice ate significantly more than the WT mice between 8 and 24 h (overnight) of the refeeding period (Fig. 1D), which corresponded to the nighttime feeding. No significant differences in body weight were found between genotypes [fasted body weight: 22.8 ± 0.7 g (WT) *vs.* 22.1 ± 0.8 g (KO), $P = 0.5$; refed body weight: 26.1 ± 0.8 (WT) *vs.* 26.2 ± 0.7 (KO), $P = 0.98$)].

Ucn 3 mutant mice had similar EE as WT littermates

Indirect calorimetry analysis was carried out to determine whether Ucn 3 mutant mice had alterations in EE. Consistent with the basal feeding study, food intake measured by metabolic cage also showed the mutant mice ate significantly more than the WT littermates (WT, 3.6 ± 0.2 *vs.* KO, 4.5 ± 0.3

TABLE 1. Endocrine and metabolic parameters of Ucn 3 WT and KO mice

	Ucn 3 WT	Ucn 3 KO	*P* value
Insulin (pg/ml)	671.7 ± 143.5	331.8 ± 74.1	0.04
Glucagon (pg/ml)	244.4 ± 58.1	204 ± 40.6	0.2
Leptin (pg/ml)	312.5 ± 130	532.2 ± 141.6	0.28
Corticosterone (ng/ml)	48.9 ± 17.2	52.2 ± 19.1	0.86
Glucose (mg/dl)	137.3 ± 10.8	131 ± 5	0.78
TG (mg/dl)	70.2 ± 7.3	64.5 ± 8.8	0.62
FFA (mg/dl)	0.57 ± 0.1	0.56 ± 0.08	0.99
Glycerol (mg/dl)	46.8 ± 8.2	40.4 ± 3.5	0.48

g/d; $P < 0.05$). On the other hand, no significant differences were observed in oxygen consumption, heat production, or activity levels between the two genotypes (Supplemental Table 3).

Blood chemistry of Ucn 3 mutant mice and WT controls

Plasma levels of insulin, glucagon, leptin, and nutrients were determined in the mutant and WT littermates, and it was found that insulin levels were significantly lower in the mutant mice than those of the WT mice (Table 1). No significant differences were found in other measurements between the two genotypes (Table 1).

GTT and ITT in Ucn 3 mutant and WT littermates

To determine whether Ucn 3 deletion results in alteration in glucose homeostasis, GTT and ITT were performed in the Ucn 3 null and WT mice. As shown in Fig. 1, E and F, Ucn 3 null and WT mice had comparable glucose tolerance and insulin sensitivity. In an ITT, the Ucn 3 null mice had a greater rebound in blood glucose levels compared with the control mice after the initial hypoglycemic response to insulin injection (Fig. 1F). Two-way ANOVA analysis revealed that genotype had a significant effect on blood glucose response to insulin injection [$F_{(1,14)} = 9.6$, $P = 0.007$].

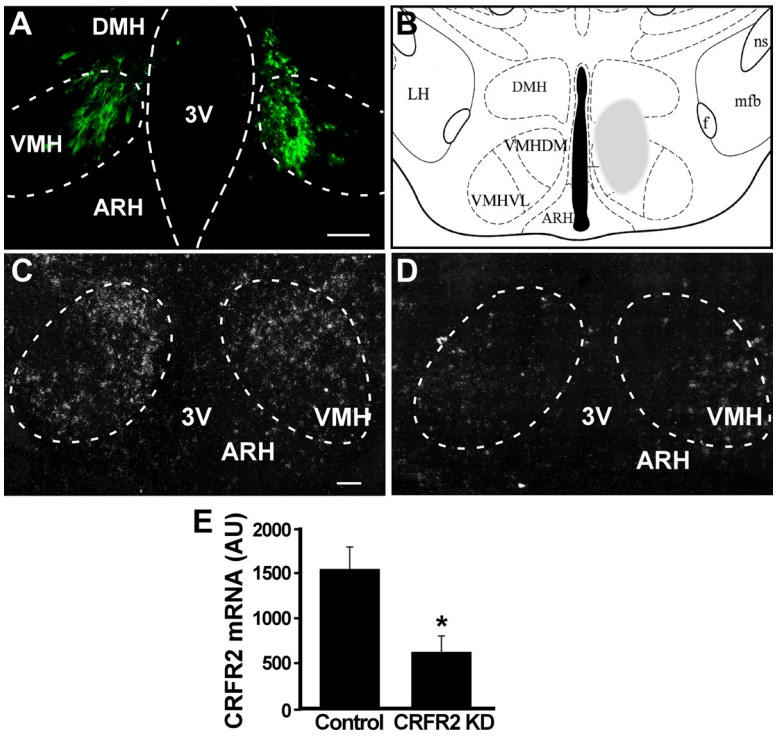

FIG. 2. Lentiviral shRNA KD CRFR2 expression in the VMH. A, Representative fluorescent image showing GFP expression in the VMH of a CRFR2 shRNA viral vector injected mouse. The location of the injection site is indicated by *shaded area* in B. C and D, Representative photomicrographs showing CRFR2 mRNA signals in control-injected (C) and CRFR2 shRNA vector-injected (D) mice in the VMH. E, Summary of CRFR2 mRNA levels in the VMH in mice injected with either control or CRFR2 shRNA viral vector into the VMH. *, $P < 0.05$. *vs.* control. *Scale bar*, 100 μm. 3V, Third ventricle; ARH, arcuate nucleus of hypothalamus; DMH, dorsomedial nucleus of hypothalamus; f, fornix; LH, lateral hypothalamus; mfb, medial forebrain bundle; ns, nigrostriatal bundle; VMHDM, dorsomedial part of VMH; VMHVL, ventrolateral part of VMH; AU, arbitrary unit.

Effects of CRFR2 KD in the VMH on basal food intake

To determine whether CRFR2 in the VMH mediates the effects of Ucn 3 in feeding and energy homeostasis, lentiviral vector expressing CRFR2 shRNA or control viral vector was injected bilaterally into the VMH of male mice (Fig. 2). Histological examination showed no apparent lesions in the VMH area (Supplemental Fig. 2). *In situ* hybridization for CRFR2 mRNA showed that mice with CRFR2 shRNA expressing viral vector injection resulted in an approximately 65% reduction in CRFR2 mRNA expression in the VMH compared with that of the control mice (Fig. 2). Food intake was measured daily for 7 d after the mice had recovered from the viral injection for 1 wk. CRFR2 KD mice showed a significant increase in average food intake over the control mice (Fig. 3A).

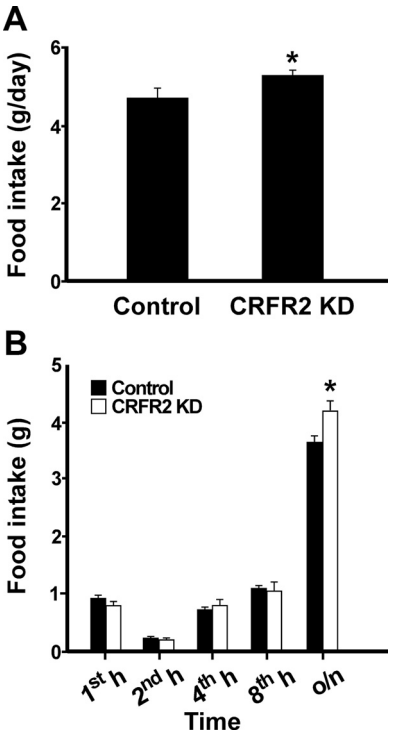

FIG. 3. Feeding response of mice with reduced CRFR2 expression in the VMH. A, Average daily food intake of mice injected with control (n = 7) or CRFR2 shRNA viral vector (CRFR2 KD; n = 6) in the VMH. B, Overnight fasting-induced feeding in control-injected (n = 6) and CRFR2 shRNA viral vector-injected (n = 6) mice. Mice were food deprived overnight, and then food intake was measured 1, 2, 4, 8, and 24 h after food was returned to the animals. o/n, Overnight. *, $P < 0.05$ *vs.* control.

Fasting-induced feeding in VMH CRFR2 KD mice and control mice

The importance of VMH CRFR2 in regulating feeding was also assessed in an overnight fasting-induced feeding paradigm. Two-way ANOVA analysis showed that although treatment alone had no effect on refeeding response [$F_{(1,10)} = 0.84$, $P = 0.38$], a significant interaction between treatment and time on overall refeeding response was observed [$F_{(4,40)} = 5.09$, $P < 0.01$]. Similar to the Ucn 3 null mice, both CRFR2 KD and control mice ate a similar amount of food at 1, 2, 4, and 8 h after onset of feeding (Fig. 3B), but the CRFR2 KD mice ate significantly more than the control mice between 8 and 24 h (overnight) of the refeeding period (Fig. 3B).

VMH CRFR2 KD mice gained more weight than the control mice

The body weight of both VMH CRFR2 KD and control mice was followed for 36 d after viral injection, and it was found that the VMH CRFR2 KD mice gained significantly more weight than the controls during the experimental period (Fig. 4A). Two-way ANOVA analysis with repeated measurement found significant effects of the treatment [$F_{(1,11)} = 4.98$, $P = 0.04$] and treatment by time interaction on body weight changes [$F_{(10,110)} = 4.03$, $P < 0.01$]. Body composition analysis showed the VMH CRFR2 KD mice had significantly more fat mass than the controls (Fig. 4B). Consistent with the body composition result, postmortem analysis at the end of the experiment showed WAT was significantly heavier in the KD mice than in the controls (Fig. 4C), whereas no differences in the weight of BAT (Fig. 4C), liver, heart, or kidney were observed (data not shown). Adipocytes of eWAT were further examined histologically. As shown in Fig. 4, D–F, the average adipocyte size was greater in the KD mice than in the control mice. Also, the mRNA levels of hormone-sensitive lipase (HSL) (control *vs.* CRFR2 KD, $P = 0.05$) and peroxisome proliferator-activated receptor (PPAR)γ1 (control *vs.* CRFR2 KD, $P = 0.04$) in the WAT were reduced in KD mice compared with the controls (Supplemental Table 4). A number of metabolic related genes was examined in the liver and muscle of the KD and control mice, and no differences were observed (Supplemental Table 4). Uncoupling protein 1 (UCP1) expression in BAT of the KD mice showed a trend toward an increase compared with that of controls, but the differences were not statistically significant ($P = 0.08$) (Supplemental Table 4).

EE in VMH CRFR2 KD and control mice

Indirect calorimetry was performed to determine whether CRFR2 KD in the VMH affects EE. As shown in Table 2, oxygen consumption was lower in VMH CRFR2 KD mice compared with that of controls when the result was normalized with body weight (3437.7 $\pm$ 63.6 *vs.* 3837.9 $\pm$ 77 ml/kg; $P < 0.05$). However, the differences were not statistically significant when oxygen consumption was normalized with lean mass (Table 2). Respiratory exchange ratio of the CRFR2 KD mice was significantly greater than that of controls (Table 2). Consistent with basal feeding study, food intake measurement showed that the VMH CRFR2 KD mice ate significantly more than the control mice (Table 2). No significant differences were found in heat production and activity levels between the two groups (Table 2).

Blood chemistry profile

Plasma levels of insulin, glucagon, and leptin were determined in controls and CRFR2 KD mice. Consistent with an increase in WAT adiposity, plasma levels of leptin in the KD mice were significantly higher than the controls (Table 3). On the other hand, circulating glucagon levels were significantly lower in the mice with CRFR2 KD than those of controls (Table 3). Circulating insulin levels were similar between the two groups. Plasma levels of catecholamines were measured to determine overall SNS

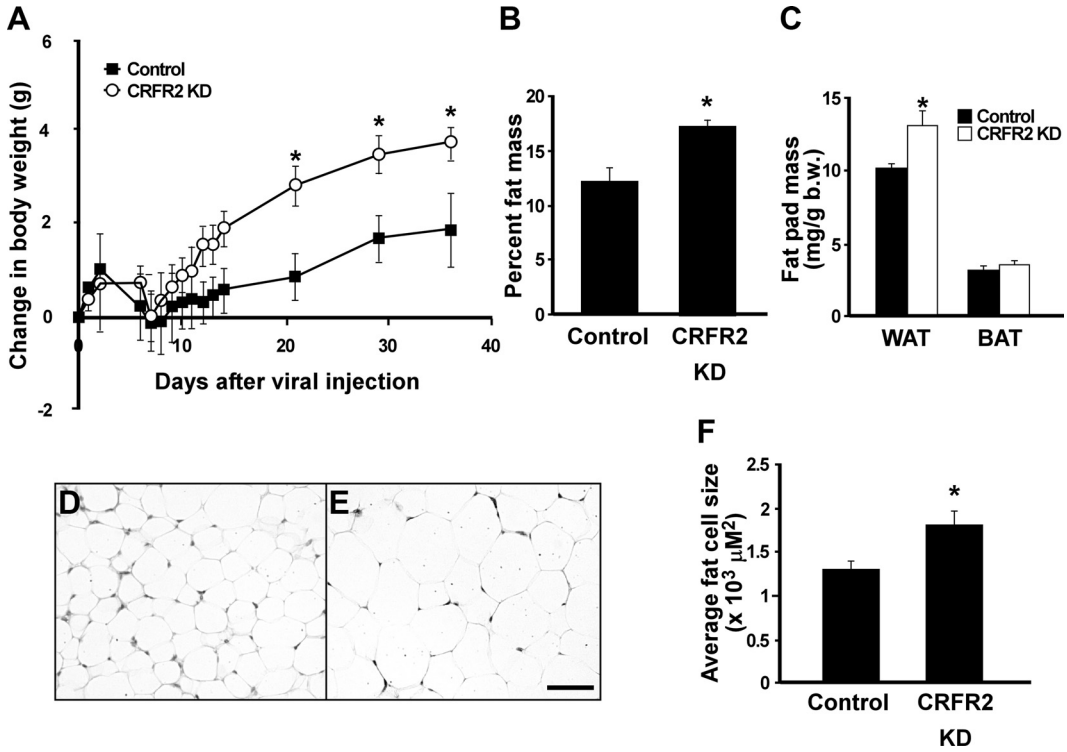

FIG. 4. Changes in body weight (A), fat mass (B), and fat pad weight (C) in mice injected with either control (n = 7) or CRFR2 shRNA (CRFR2 KD) viral vector (n = 6). D and E, Representative photomicrographs showing hematoxylin and eosin-stained eWAT section of control (D) or CRFR2 KD (E) mice. F, Summary of average fat cell size in eWAT of control and CRFR2 KD mice. *, $P < 0.05$ *vs.* control.

activity. It was found that plasma levels of catecholamines in the CRFR2 KD mice showed a trend toward lower than that of control mice, although the differences were not statistically significant. The increase in WAT weight in CRFR2 KD mice suggested that lipolysis in WAT may be reduced in KD mice. Consistent with this notion, plasma levels of FFA and glycerol were significantly lower in KD mice compared with control mice (Table 3). No differences were found in plasma triglyceride (TG) and glucose levels between the two groups (Table 3).

VMH CRFR2 KD improves glucose homeostasis

To examine whether reduced CRFR2 expression in the VMH impacts glucose homeostasis, a GTT was performed in VMH CRFR2 KD and control mice. As shown in Fig. 5A, the VMH CRFR2 KD mice exhibited improved GTT compared with the control mice. Two-way ANOVA analysis found significant effects of treatment [$F_{(1,8)} = 6.7$, $P = 0.03$] and treatment by time interaction [$F_{(5,40)} = 5.3$, $P < 0.001$] on blood glucose levels. An ITT was also performed to further examine the effect of VMH CRFR2 KD on insulin sensitivity (Fig. 5B). Two-way ANOVA analysis with repeated measurement revealed that blood glucose response to insulin injection was independent of treatment [$F_{(1,10)} = 0.54$, $P = 0.48$], but a significant interaction between treatment and time was observed [$F_{(5,40)} = 10.9$, $P < 0.001$]. It was found that the CRFR2 KD mice had significantly lower blood glucose levels than the control mice 15 min after insulin injection (Fig. 5B).

TABLE 2. Indirect calorimetry analysis of VMH CRFR2 shRNA and control viral vector injected mice

	Control	CRFR2 shRNA	*P* value
VO2 (ml/kg · h)	3837.9 ± 77.1	3493. ± 63.6	0.01
VO2 (ml/kg lean mass/h)	4605.4 ± 127.8	4330.5 ± 91.7	0.13
VCO2 (ml/kg · h)	3294.9 ± 55.3	3187.3 ± 85.1	0.28
RMR (ml/kg · h)	3014.5 ± 76.2	2715.5 ± 90.63	0.03
RER	0.83 ± 0.005	0.88 ± 0.01	0.0004
Heat production (kcal/kg)	0.52 ± 0.02	0.53 ± 0.01	0.84
Food (g/d)	3.91 ± 0.12	4.68 ± 0.2	0.002
Drink (ml/d)	3.89 ± 0.34	3.36 ± 0.15	0.23
Activity (counts)	527.9 ± 100.4	468.7 ± 50.9	0.64

RER, Respiratory exchange ratio; RMR, resting metabolic rate. VO_2, oxygen consumption; VCO_2, carbon dioxide production.

TABLE 3. Endocrine and metabolic parameters of mice injected with control or CRFR2 shRNA viral vector

	Control	CRFR2 shRNA	*P* value
Insulin (pg/ml)	667.8 ± 156	727.5 ± 64.9	0.39
Glucagon (pg/ml)	251.2 ± 8.5	203.3 ± 19.4	0.044
Leptin (pg/ml)	172.8 ± 19.8	362.2 ± 50	0.008
Corticosterone (ng/ml)	37.2 ± 5.9	21.4 ± 6.6	0.1
Epinephrine (pg/ml)	91.1 ± 33.8	70 ± 31.4	0.6
Norepinephrine (pg/ml)	745.6 ± 181.7	544.9 ± 161.3	0.4
Glucose (mg/dl)	114.5 ± 4.6	136.5 ± 10.3	0.08
TG (mg/dl)	62.9 ± 6	60.1 ± 3.4	0.7
FFA (mg/dl)	1.56 ± 0.06	1.1 ± 0.07	0.0009
Glycerol (mg/dl)	67.4 ± 4.6	46.7 ± 3.4	0.002

Similar to Ucn 3 null mice, CRFR2 KD mice had a greater rebound in blood glucose levels compared with control mice after the initial hypoglycemic response to insulin injection (Fig. 5B).

Discussion

The function of central Ucn 3 in regulating feeding, SNS activity, and blood glucose levels is well documented (8–10). In the present study, we show the Ucn 3 mutant mice displayed a significant elevation in basal food intake compared with the WT littermates. Similar to Ucn 3-deficient mice, mice with CRFR2 KD in the VMH also exhibited elevation in basal feeding compared with control mice. Thus, these results provide the first evidence that endogenous Ucn 3 is involved in regulating feeding, and the effect of Ucn 3 in feeding is likely mediated centrally by CRFR2 in the VMH.

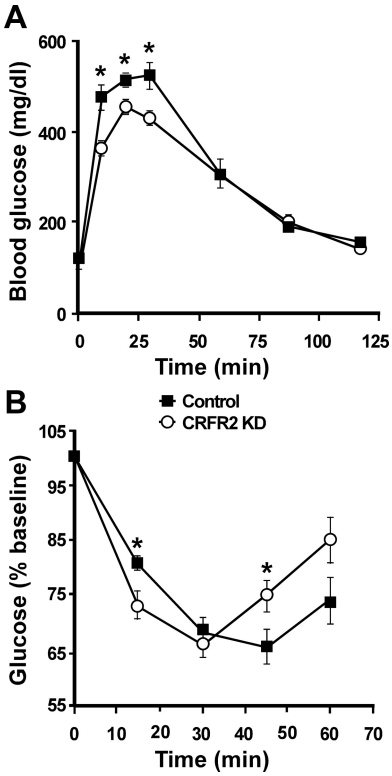

FIG. 5. GTT (A) and ITT (B) in mice received either control (n = 6) or CRFR2 shRNA (CRFR2 KD) viral vector (n = 6) injection into the VMH. Glucose (2 g/kg body weight) or insulin (0.75 IU/kg body weight) was injected ip, and blood glucose was measured at various time points. *, $P < 0.05$ *vs.* control.

In addition to basal food intake, the importance of endogenous Ucn 3 in regulating appetite was examined with an overnight fasting-induced refeeding paradigm. Although Ucn 3 null mice showed an early phase of refeeding response comparable with the WT littermates, the mutant mice had elevated dark-phase feeding compared with the WT mice. This result indicates that endogenous Ucn 3 is important in regulating nocturnal feeding when the greatest spontaneous food intake occurs. Moreover, VMH CRFR2 KD mice also showed similar refeeding responses as Ucn 3 null mice, further supporting the hypothesis that function of endogenous Ucn 3 in feeding is mediated by VMH CRFR2. It has been shown that CRFR2 null mice display elevated night-time feeding (34). This increase in nocturnal food intake of CRFR2 null mice is mainly due to an increase in meal size but not meal frequency, suggesting a decreased satiating value of food (34). Interestingly, mice deficient in Ucn 2, another endogenous ligand for CRFR2 (35), do not exhibit enhancement in nocturnal food intake (36). Taken together, these data argue that Ucn 3 acting through CRFR2 in the VMH is an important signal involved in terminating feeding.

In the present study, we found that reduced expression of CRFR2 in the VMH resulted in significant weight gain due to an increase in WAT mass, whereas no differences in other organs were found. Consistent with the increase in WAT mass, circulating leptin, which is known to be proportional to fat mass (37–40), of the KD mice was significantly elevated compared with controls. Reduced CRFR2 expression in the VMH has no apparent impact on EE, because no differences in EE per lean mass, activity levels, and heat production were observed between the VMH CRFR2 KD mice and controls. Obviously, increased calorie intake likely contributes to the weight gain

observed in CRFR2 KD mice. In addition to hyperphagia, our data suggest that alteration in lipid metabolism in WAT of VMH CRFR2 KD mice also contributes to increased WAT adiposity. Histological examination revealed that the average size of fat cells in WAT of the VMH CRFR2 KD mice was significantly increased compared with that of control mice. In addition, compared with control mice, the receptor KD mice had significantly lower circulating FFA and glycerol levels and a higher respiratory exchange ratio. These data suggest that suppression of VMH CRFR2 expression results in reduced lipolysis in WAT. Electrical stimulation of VMH leads to elevation of lipolysis of WAT, and this effect of VMH on WAT lipolysis is mediated by the SNS (27). On the other hand, lesions of the VMH have been associated with reduced lipolysis in WAT (29). Finally, the hypothalamus does not appear to play a significant role in FFA clearance from the plasma (41). Taken together, our study suggests that CRFR2 signaling is a critical molecular mediator in the VMH in modulating WAT mass through lipolysis.

In addition to a decrease in circulating FFA and glycerol levels, the expression of HSL in WAT of VMH CRFR2 KD mice was greatly reduced compared with that of controls, consistent with the hypothesis that lipolysis is reduced in the WAT of KD mice. In addition to HSL, PPARγ1 mRNA levels were significantly suppressed in the KD mice compared with control mice. It has been shown that PPARγ promotes the expression of lipolytic enzymes, including HSL and TG lipase in fat cells (42, 43). Our study suggests that chronic suppression of SNS outflow into WAT leads to a reduction in expression of genes important for lipolysis and subsequently lower basal lipolytic activity in WAT.

Earlier studies have found that total CRFR2 KO mice had increased thermogenesis, greatly elevated UCP1 expression in BAT, and smaller adipocyte size in WAT and BAT compared with WT mice (44, 45). In the present study, VMH CRFR2 KD results in a subtle increase in BAT UCP1 expression and enlarged adipocytes in WAT, in contrast to reduced fat cell size reported in total CRFR2 KO mice. It has been postulated that the phenotypes observed in total CRFR2 KO mice are due to a compensatory elevation of central CRFR1 activity, because CRFR2 null mice have an elevated expression of CRFR1 preferred ligands (CRF and Ucn 1) in the brain (46). The elevated CRFR1 activity leads to increased SNS activity in BAT, which may then increase usage of serum lipid, depleting WAT and BAT stores and decreasing adipose cell size (45). Thus, the discrepancies between total CRFR2 deletion and VMH CRFR2 KD may be due, in part, to differences in CRFR1 activity in these two animal models.

An interesting observation in the present study was that the Ucn 3 null mice showed comparable body weight as the WT littermates in the face of hyperphagia. Ucn 3 null mice exhibited comparable EE, heat production, and activity levels with the WT littermates, ruling out the possibility that elevation of EE offset increase in energy intake. Importantly, similar phenotype (hyperphagia while maintaining similar weight as WT) has been observed in mice deficient in CRFR2 under high-fat diet (HFD), and it was attributed to elevated thermogenesis in BAT (45). Thus, although the mechanism by which Ucn 3 null mice consumed substantially more food while maintaining similar weight as WT mice remains to be determined, the possibility that an elevated thermogenesis in Ucn 3 null mice to offset increased energy intake cannot be ruled out.

The role of endogenous Ucn 3 in regulating glucose homeostasis has been examined previously under HFD conditions (30). It was found that abrogating endogenous Ucn 3 protects mice from HFD induced insulin resistance, because the mutant mice remained insulin sensitive under HFD feeding compared with WT littermates (30). Our study shows that Ucn 3 mutant and WT mice under normal chow diet displayed comparable glucose tolerance and insulin sensitivity. Taken together, these data suggest that endogenous Ucn 3 plays a critical role in glucose homeostasis under excessive caloric conditions. However, the specific role and contribution of different sources of Ucn 3 to glucose homeostasis remain unclear. In the present study, mice with reduced VMH CRFR2 expression showed improved glucose homeostasis compared with control mice. Consistent with our result, direct Ucn 3 injection into the VMH rapidly elevates blood glucose levels (13) and overexpression of Ucn 3 in the hypothalamus results in reduced insulin sensitivity (12). These data support the notion that VMH CRFR2 neurons play an important role in regulating glucose homeostasis. Currently, it is not clear how VMH CRFR2 neurons modulate peripheral insulin sensitivity. It has been shown that elevated FFA reduce insulin sensitivity and lead to insulin resistance (47, 48). On the other hand, genetic mouse models with decreased circulating FFA preferred carbohydrate as an energy source and exhibited improved glucose tolerance and insulin sensitivity (49). Thus, we speculate that enhanced insulin sensitivity in VMH CRFR2 KD mice may be attributed, at least in part, to reduced circulating FFA and glycerol levels in these mice.

A striking similarity was observed in Ucn 3 null and VMH CRFR2 KD mice in the ITT, because both groups exhibited an exaggerated rebound in blood glucose levels compared with the respective control mice after the initial hypoglycemic response to insulin injection. This result suggests that endogenous Ucn 3 in the VMH has an

inhibitory effect in hypoglycemia-induced counterregulatory response (CRR). Consistent with our finding, McCrimmon *et al*. (50) have shown that injection of Ucn 3 into the VMH suppresses hypoglycemia-induced glucagon and catecholamine secretion. This effect appears to be associated with hypoglycemia, because Ucn 3 injection into the VMH under euglycemia rapidly elevates blood glucose levels (13), and activation of CRFR2 blunts VMH glucose sensing neuron activity only when extracellular glucose levels were lowered to hypoglycemic conditions (50). Taken together, our data demonstrate that endogenous Ucn 3 through CRFR2 in the VMH plays a critical role in regulating hypoglycemia-induced CRR response. It will be particularly important to determine whether this system is involved in a defective CRR response to recurrent hypoglycemia commonly found in type 1 diabetes (50).

In conclusion, our study demonstrates that endogenous Ucn 3, through CRFR2 in the VMH, is a critical molecular mediator in regulating multiple physiological functions, including feeding, lipolysis in WAT, and hypoglycemia-induced CRR.

Acknowledgments

We thank Dan Lindberg for providing technical assistance in RNA extraction and real-time PCR analysis and David Lin for providing assistance in brain sectioning and *in situ* hybridization. We also thank Dr. Jae Lee and Dr. Wenjun Xin for providing assistance in statistical analysis and Dr. Michael Thorner, Dr. Thurl Harris, and Dr. Michael Scott for providing comments on the manuscript.

Address all correspondence and requests for reprints to: Chien Li, Ph.D., Department of Pharmacology, P.O. Box 800735, University of Virginia Health System, Charlottesville, Virginia 22903. E-mail: cl4xd@virginia.edu.

This work was supported by the National Institute of Diabetes and Digestive and Kidney Diseases Grant R01 DK-078049 (to C.L.).

Disclosure Summary: The authors have nothing to disclose.

References

1. **Lewis K, Li C, Perrin MH, Blount A, Kunitake K, Donaldson C, Vaughan J, Reyes TM, Gulyas J, Fischer W, Bilezikjian L, Rivier J, Sawchenko PE, Vale WW** 2001 Identification of urocortin III, an additional member of the corticotropin-releasing factor (CRF) family with high affinity for the CRF2 receptor. Proc Natl Acad Sci USA 98:7570–7575
2. **Hsu SY, Hsueh AJ** 2001 Human stresscopin and stresscopin-related peptide are selective ligands for the type 2 corticotropin-releasing hormone receptor. Nat Med 7:605–611
3. **Li C, Vaughan J, Sawchenko PE, Vale WW** 2002 Urocortin III-immunoreactive projections in rat brain: partial overlap with sites of type 2 corticotrophin-releasing factor receptor expression. J Neurosci 22:991–1001
4. **Li C, Chen P, Vaughan J, Blount A, Chen A, Jamieson PM, Rivier J, Smith MS, Vale W** 2003 Urocortin III is expressed in pancreatic β-cells and stimulates insulin and glucagon secretion. Endocrinology 144:3216–3224
5. **Takahashi K, Totsune K, Saruta M, Fukuda T, Suzuki T, Hirose T, Imai Y, Sasano H, Murakami O** 2006 Expression of urocortin 3/stresscopin in human adrenal glands and adrenal tumors. Peptides 27:178–182
6. **Takahashi K, Totsune K, Murakami O, Saruta M, Nakabayashi M, Suzuki T, Sasano H, Shibahara S** 2004 Expression of urocortin III/stresscopin in human heart and kidney. J Clin Endocrinol Metab 89:1897–1903
7. **Saruta M, Takahashi K, Suzuki T, Fukuda T, Torii A, Sasano H** 2005 Urocortin 3/stresscopin in human colon: possible modulators of gastrointestinal function during stressful conditions. Peptides 26:1196–1206
8. **Jamieson PM, Li C, Kukura C, Vaughan J, Vale W** 2006 Urocortin 3 modulates the neuroendocrine stress response and is regulated in rat amygdala and hypothalamus by stress and glucocorticoids. Endocrinology 147:4578–4588
9. **Fekete EM, Inoue K, Zhao Y, Rivier JE, Vale WW, Szücs A, Koob GF, Zorrilla EP** 2007 Delayed satiety-like actions and altered feeding microstructure by a selective type 2 corticotropin-releasing factor agonist in rats: intra-hypothalamic urocortin 3 administration reduces food intake by prolonging the post-meal interval. Neuropsychopharmacology 32:1052–1068
10. **Ohata H, Shibasaki T** 2004 Effects of urocortin 2 and 3 on motor activity and food intake in rats. Peptides 25:1703–1709
11. **Pelleymounter MA, Joppa M, Ling N, Foster AC** 2004 Behavioral and neuroendocrine effects of the selective CRF2 receptor agonists urocortin II and urocortin III. Peptides 25:659–666
12. **Kuperman Y, Issler O, Regev L, Musseri I, Navon I, Neufeld-Cohen A, Gil S, Chen A** 2010 Perifornical urocortin-3 mediates the link between stress-induced anxiety and energy homeostasis. Proc Natl Acad Sci USA 107:8393–8398
13. **Chen P, Vaughan J, Donaldson C, Vale WW, Li C** 2010 Injection of Urocortin 3 into the ventromedial hypothalamus modulates feeding, blood glucose levels and hypothalamic POMC gene expression but not the HPA axis. Am J Physiol 298:E337–E345
14. **Chalmers DT, Lovenberg TW, De Souza EB** 1995 Localization of novel corticotropin-releasing factor receptor (CRF_2) mRNA expresssion to specific subcortical nuclei in rat brain: comparison with CRF_1 receptor mRNA expression. J Neurosci 15:6340–6350
15. **Van Pett K, Viau V, Bittencourt JC, Chan RK, Li HY, Arias C, Prins GS, Perrin M, Vale W, Sawchenko PE** 2000 Distribution of mRNAs encoding CRF receptors in brain and pituitary of rat and mouse. J Comp Neurol 428:191–212
16. **King BM** 2006 The rise, fall, and resurrection of the ventromedial hypothalamus in the regulation of feeding behavior and body weight. Physiol Behav 87:221–244
17. **Jacob RJ, Dziura J, Medwick MB, Leone P, Caprio S, During M, Shulman GI, Sherwin RS** 1997 The effect of leptin is enhanced by microinjection into the ventromedial hypothalamus. Diabetes 46:150–152
18. **Satoh N, Ogawa Y, Katsuura G, Tsuji T, Masuzaki H, Hiraoka J, Okazaki T, Tamaki M, Hayase M, Yoshimasa Y, Nishi S, Hosoda K, Nakao K** 1997 Pathophysiological significance of the obese gene product, leptin, in ventromedial hypothalamus (VMH)-lesioned rats: evidence for loss of its satiety effect in VMH-lesioned rats. Endocrinology 138:947–954
19. **Dhillon H, Zigman JM, Ye C, Lee CE, McGovern RA, Tang V, Kenny CD, Christiansen LM, White RD, Edelstein EA, Coppari R, Balthasar N, Cowley MA, Chua Jr S, Elmquist JK, Lowell BB** 2006 Leptin directly activates SF1 neurons in the VMH, and this action by

leptin is required for normal body-weight homeostasis. Neuron 49: 191–203
20. **Avrith D, Mogenson GJ** 1978 Reversible hyperphagia and obesity following intracerebral microinjections of colchicine into the ventromedial hypothalamus of the rat. Brain Res 153:99–107
21. **Kim KW, Zhao L, Donato Jr J, Kohno D, Xu Y, Elias CF, Lee C, Parker KL, Elmquist JK** 2011 Steroidogenic factor 1 directs programs regulating diet-induced thermogenesis and leptin action in the ventral medial hypothalamic nucleus. Proc Natl Acad Sci USA 108: 10673–10678
22. **Perkins MN, Rothwell NJ, Stock MJ, Stone TW** 1981 Activation of brown adipose tissue thermogenesis by the ventromedial hypothalamus. Nature 289:401–402
23. **Kang L, Routh VH, Kuzhikandathil EV, Gaspers LD, Levin BE** 2004 physiological and molecular characteristics of rat hypothalamic ventromedial nucleus glucosensing neurons. Diabetes 53:549–559
24. **Tong Q, Ye C, McCrimmon RJ, Dhillon H, Choi B, Kramer MD, Yu J, Yang Z, Christiansen LM, Lee CE, Choi CS, Zigman JM, Shulman GI, Sherwin RS, Elmquist JK, Lowell BB** 2007 synaptic glutamate release by ventromedial hypothalamic neurons is part of the neurocircuitry that prevents hypoglycemia. Cell Metab 5:383–393
25. **Miki T, Liss B, Minami K, Shiuchi T, Saraya A, Kashima Y, Horiuchi M, Ashcroft F, Minokoshi Y, Roeper J, Seino S** 2001 ATP-sensitive K+ channels in the hypothalamus are essential for the maintenance of glucose homeostasis. Nat Neurosci 4:507–512
26. **Kumon A, Takahashi A, Hara T, Shimazu T** 1976 Mechanism of lipolysis induced by electrical stimulation of the hypothalamus in the rabbit. J Lipid Res 17:551–558
27. **Takahashi A, Shimazu T** 1981 Hypothalamic regulation of lipid metabolism in the rat: effect of hypothalamic stimulation on lipolysis. J Auton Nerv Syst 4:195–205
28. **Ruffin M, Nicolaidis S** 1999 Electrical stimulation of the ventromedial hypothalamus enhances both fat utilization and metabolic rate that precede and parallel the inhibition of feeding behavior. Brain Res 846:23–29
29. **Bray GA, Nishizawa Y** 1978 Ventromedial hypothalamus modulates fat mobilisation during fasting. Nature 274:900–902
30. **Li C, Chen P, Vaughan J, Lee KF, Vale W** 2007 Urocortin 3 regulates glucose-stimulated insulin secretion and energy homeostasis. Proc Natl Acad Sci USA 104:4206–4211
31. **Tiscornia G, Singer O, Verma IM** 2006 Production and purification of lentiviral vectors. Nat Protoc 1:241–245
32. **Brar BK, Chen A, Perrin MH, Vale W** 2004 Specificity and regulation of extracellularly regulated kinase1/2 phosphorylation through corticotropin-releasing factor (CRF) receptors 1 and 2β by the CRF/urocortin family of peptides. Endocrinology 145:1718–1729
33. **Livak KJ, Schmittgen TD** 2001 Analysis of relative gene expression data using real-time quantitative PCR and the $2(-\Delta\Delta C(T))$ method. Methods 25:402–408
34. **Tabarin A, Diz-Chaves Y, Consoli D, Monsaingeon M, Bale TL, Culler MD, Datta R, Drago F, Vale WW, Koob GF, Zorrilla EP, Contarino A** 2007 Role of the corticotropin-releasing factor receptor type 2 in the control of food intake in mice: a meal pattern analysis. Eur J Neurosci 26:2303–2314
35. **Reyes TM, Lewis K, Perrin MH, Kunitake KS, Vaughan J, Arias CA, Hogenesch JB, Gulyas J, Rivier J, Vale WW, Sawchenko PE** 2001 Urocortin II: a member of the corticotropin-releasing factor (CRF) neuropeptide family that is selectively bound by type 2 CRF receptors. Proc Natl Acad Sci USA 98:2843–2848
36. **Chen A, Zorrilla E, Smith S, Rousso D, Levy C, Vaughan J, Donaldson C, Roberts A, Lee KF, Vale W** 2006 Urocortin 2-deficient mice exhibit gender-specific alterations in circadian hypothalamus-pituitary-adrenal axis and depressive-like behavior. J Neurosci 26: 5500–5510
37. **Considine RV, Sinha MK, Heiman ML, Kriauciunas A, Stephens TW, Nyce MR, Ohannesian JP, Marco CC, McKee LJ, Bauer TL, *et al*.** 1996 Serum immunoreactive-leptin concentrations in normal-weight and obese humans. New Engl J Med 334:292–295
38. **Havel PJ, Kasim-Karakas S, Mueller W, Johnson PR, Gingerich RL, Stern JS** 1996 Relationship of plasma leptin to plasma insulin and adiposity in normal weight and overweight women: effects of dietary fat content and sustained weight loss. J Clin Endocrinol Metab 81: 4406–4413
39. **Maffei M, Halaas J, Ravussin E, Pratley RE, Lee GH, Zhang Y, Fei H, Kim S, Lallone R, Ranganathan S** 1995 Leptin levels in human and rodent: measurement of plasma leptin and ob RNA in obese and weight-reduced subjects. Nat Med 1:1155–1161
40. **McGregor GP, Desaga JF, Ehlenz K, Fischer A, Heese F, Hegele A, Lammer C, Peiser C, Lang RE** 1996 Radiommunological measurement of leptin in plasma of obese and diabetic human subjects. Endocrinology 137:1501–1504
41. **Barkai A, Allweis C** 1975 Transport of plasma FFA in cats; effect of hypothalamic stimulation. Am J Physiol 228:1367–1375
42. **Kershaw EE, Schupp M, Guan HP, Gardner NP, Lazar MA, Flier JS** 2007 PPARγ regulates adipose triglyceride lipase in adipocytes in vitro and in vivo. Am J Physiol 293:E1736–E1745
43. **Deng T, Shan S, Li PP, Shen ZF, Lu XP, Cheng J, Ning ZQ** 2006 Peroxisome proliferator-activated receptor-γ transcriptionally up-regulates hormone-sensitive lipase via the involvement of specificity protein-1. Endocrinology 147:875–884
44. **Carlin KM, Vale WW, Bale TL** 2006 Vital functions of corticotropin-releasing factor (CRF) pathways in maintenance and regulation of energy homeostasis. Proc Natl Acad Sci USA 103:3462–3467
45. **Bale TL, Anderson KR, Roberts AJ, Lee KF, Nagy TR, Vale WW** 2003 Corticotropin-releasing factor receptor-2-deficient mice display abnormal homeostatic responses to challenges of increased dietary fat and cold. Endocrinology 144:2580–2587
46. **Bale TL, Contarino A, Smith GW, Chan R, Gold LH, Sawchenko PE, Koob GF, Vale WW, Lee KF** 2000 Mice deficient for corticotropin-releasing hormone receptor-2 display anxiety-like behaviour and are hypersensitive to stress. Nature Genetics 24:410–414
47. **Eckardt K, Taube A, Eckel J** 2011 Obesity-associated insulin resistance in skeletal muscle: role of lipid accumulation and physical inactivity. Rev Endocr Metab Dis 12:163–172
48. **Bergman RN, Ader M** 2000 Free fatty acids and pathogenesis of type 2 diabetes mellitus. Trends Endocrinol Metab 11:351–356
49. **Zimmermann R, Strauss JG, Haemmerle G, Schoiswohl G, Birner-Gruenberger R, Riederer M, Lass A, Neuberger G, Eisenhaber F, Hermetter A, Zechner R** 2004 Fat mobilization in adipose tissue is promoted by adipose triglyceride lipase. Science 306:1383–1386
50. **McCrimmon RJ, Song Z, Cheng H, McNay EC, Weikart-Yeckel C, Fan X, Routh VH, Sherwin RS** 2006 Corticotrophin-releasing factor receptors within the ventromedial hypothalamus regulate hypoglycemia-induced hormonal counterregulation. J Clin Invest 116: 1723–1730